Straining Phenomena of POY Revealed by Thermal Retraction and Other Techniques*

DROR SELIVANSKY and MENACHEM LEWIN, *Israel Fiber Institute, P.O.B. 8001, Jerusalem, Israel*

Synopsis

Partially oriented polyester yarns (POY) were strained at different strain rates (0.03–12.00 min^{-1}) and temperatures above and below T_g (3–92°C). Thermal retraction, density, DSC, and WAXS techniques show that strain-induced crystallization takes place by straining at temperatures above as well as below T_g. Above T_g, depending upon the strain rate, two regimes are observed: Below the strain rate of 1.5 min^{-1}, the flow regime; the degree of crystallinity is reduced as the strain rate increases. Above the strain rate of 1.5 min^{-1}, the strain-induced crystallization regime; the degree of crystallinity increases as the strain rate increases. Thermal retraction, stress–relaxation, and sonic modulus techniques indicate that, upon cold straining, instead of the original T_g at 65–69°C, two glass transitions occur: an upper $T_g(u)$ and a lower $T_g(l)$. For POY strained at 3°C and at a strain rate of 10 min^{-1}, the values are 78°C and 37°C, respectively. The higher the strain rate and the lower the straining temperature, the larger the difference between $T_g(u)$ and $T_g(l)$.

INTRODUCTION

In a previous investigation from this laboratory, it has been shown that thermal retraction is an excellent technique for the investigation of partially oriented polyester yarns (POY).[2] Techniques based on thermal retraction were used recently to detect structural changes of POY with changes occurring upon applying various spinning speeds,[3,4] organic solvent treatments,[5] thermal treatments,[6] texturizing,[7] and stress-induced crystallization.[8,9] Bosley's theory on fiber-length changes in relation to structure gives an explanation for the shrinkage behavior of the fibers.[10] Its principles were later experimentally confirmed.[11,2,12] The theory applies rubber elasticity principles which yield the shrinkage tension $f = T(\partial S/\partial l)_T$ in the free rotation phase. Since rotational freedom prevails only in the amorphous phase, shrinkage tension arises solely from oriented amorphous regions at $T > T_g$, when T_g is the temperature at which large enough numbers of polymeric segments possess kinetic energy to overcome the rotational barriers in the observer's time scale. Shrinkage thermograms reveal the degree of orientation of the amorphous regions, which is changed at a certain temperature in a fiber. The shrinkage thus allows an estimate of the distribution of the size and perfection of crystalline regions and is a most sensitive technique to detect crystallization and nucleation processes.[2,7–9]

Retraction thermograms give precisely the temperature of the onset of shrinkage which is related to the T_g of the fiber.[10,13] In the present study, thermal retraction was used as a major characterization technique for POY strained at different temperatures with strain rates.

While strain induced crystallization of amorphous PET has been studied over

* The present results were included in a presentation at the Israel Chemical Society in 1978.[1]

Journal of Applied Polymer Science, Vol. 27, 2337–2349 (1982)
 CCC 0021-8995/82/072337-13$02.30

a long period of time,[14-20] only recently studies on POY[3,4,21,22,8] revealed that in POY produced under conditions of high wind-up speeds, strain- and stress-induced crystallization takes place.

Several investigators[23-29] recently found for PET an additional low temperature T_g between 30°C and 60°C. Boyer[23] introduced the concept of the double T_g associated with two differently ordered amorphous phases that give higher and lower glass transitions. PET is mentioned as capable of showing this phenomenon.

Chao[24,25] discovered in PET a secondary T_g in the temperature range of 40–60°C. He related the transition to local order produced during the cold stretch process. Illers and Bruer[26] described a secondary T_g in PET at 50°C. Ito and Hatakayama[27] found a low T_g in PET correlated to the natural draw ratio of the fibers. Nicholais and Dibenedetto[28] offered an explanation for the lowering of T_g upon cold stretching of PET, i.e., microvoid formation increases the free volume.

Yau[29] found a low T_g in cold-presses PET sheets.

Both the phenomena of the strain-induced crystallization and of the lowering of the T_g in POY fibers at different rates and temperatures are investigated in this study.

EXPERIMENTAL

Materials

The POY yarns obtained from Monsanto Chemical Co., U.S.A., were 270 denier/34 filaments. The yarns were stored below 25°C.

Silicone oil, General Electric SF-96, was used as the heating medium.

Straining Apparatus

The yarns were wound in loops between hooks mounted on the two clamps of an Instron Universal Testing Instrument Model TM. The hooks with the loops were inserted into a silicone oil bath maintained at a constant temperature measured near the yarn by a thermocouple. The stretching of the yarns was done after immersion in the oil for 30 s and stress–strain curves were obtained upon drawing to the natural draw ratio. The range of the straining rates was 0.05–12.00 min^{-1}. The straining temperatures were 80°C, 90°C, above T_g, and 60°C, 21°C, 3°C, below T_g.

Thermal Retraction

The technique is described elsewhere.[2] The yarns were immersed in silicone oil and inserted by means of a monofilament loop into thin walled 5-cm-long narrow glass capillary tubes. The capillaries with the yarns were heated on a Kopler hot stage at a heating rate of 5°C/min. Dimensional changes were measured through a magnifying glass. Thermal retraction values were taken at intervals of 5°C or less.

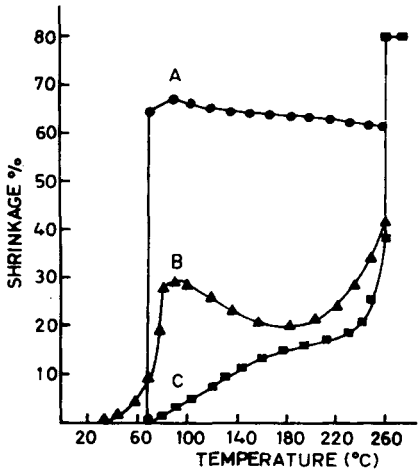

Fig. 1. Thermal retraction of the yarns: (A) Untreated POY; (B) cold-drawn POY, 1.6x at 20°C and strain rate 12.00 min^{-1}; (C) FOY hot-drawn to the natural draw ratio. Experimental error: Δs = ±0.1%, ΔT = ±0.5°C.

Density

Densities were measured in a density gradient column[30] according to ASTM D 1505-68 and BS 3715 1964 standards. A mixture of carbon tetrachloride and n-hexane gave a density range of 1.32–1.52 g/mL.

DSC

Thermograms were measured on a DSC DuPont model 900 differential scanning Analyzer. The scans were obtained at a heating rate of 10°C/min.

Relative degrees of crystallinity were calculated from the melting endotherm peak areas normalized by the samples' weights after subtraction of the crystallization exothermic peak areas. Sample sizes were ca. 5 mg.

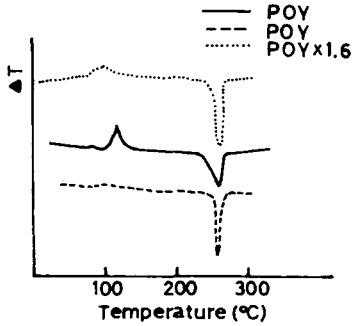

Fig. 2. DSC thermograms of the yarns: Untreated POY, FOY hot-drawn to the natural draw ratio, cold-drawn POY, POY drawn 1.6x at 20°C and strain rate 12.00 min^{-1}. Note: exothermic crystallization peak starts at 90°C in cold-drawn POY, almost disappears in FOY, and very intensive in POY (from Ref. 2).

TABLE I
WAXS Index of Crystallinity, I 25°6/I 28°6, and Index of Amorphous Phase, I 14°/I 28°6 of Samples Strained at Different Rates and Temperatures

Index of crystallinity I 25°6/I 28°6	Index of amorphous phase I 14°/I 28°6	Strain rate (min^{-1})	Temp (°C)
1.610	1.130	0.05	60
1.622	1.090	0.15	60
1.710	0.885	5.00	60
1.750	0.860	10.00	60
1.615	1.102	0.05	21
1.640	1.000	1.66	21
1.660	0.899	5.00	21
1.700	1.050	10.00	21
1.600	1.135	—	—

WAXS

Diagrams were obtained in a 1030 Philips diffractometer, using CuKα with Ni filter; λ = 1.54 Å; angular range, 2θ = 2°–45°.

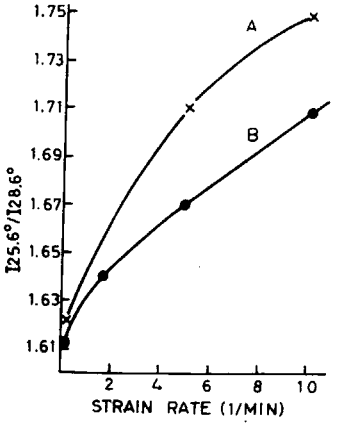

Fig. 3. Bosley's index of crystallinity vs. strain rates below T_g. Straining temperatures: (A) 60°C; (B) 21°C. Experimental error: ΔI 25°6/I 28°6 = ±0.01, Δ strain rate = ±0.1 min^{-1}.

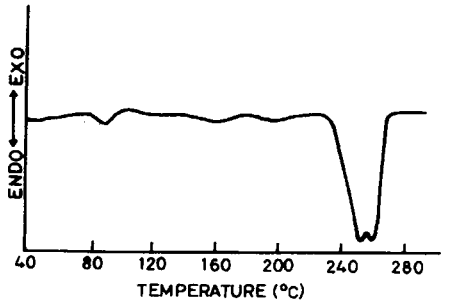

Fig. 4. DSC thermogram of POY strained at 60°C at strain rate 0.5 min^{-1}. Note: split melting peak: 254°C and 258°C. Exothermic peak is almost absent at 90°C.

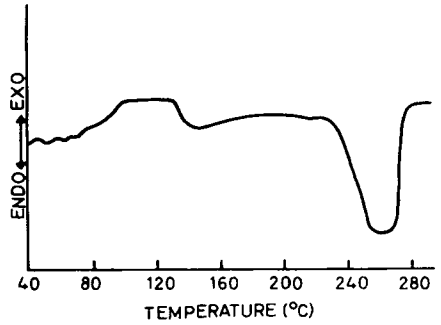

Fig. 5. DSC thermograms of POY strained at 3°C at strain rate 10.0 min^{-1}. Note: a wide endotherm with a peak at 260°C. A very wide exothermic crystallization peak starts at 90°C.

Methods used to determine the degree of crystallinity were:

(A) Bosley's index of crystallinity[31]:

$$\chi = I\ 25°6/I\ 28°6$$

where χ = degree of crystallinity, I 25°6 = intensity of (100) diffraction plane, and I 28°6 = normalizing intensity.

(B) Dumbleton's method[32]:

$$A = I\ 14°/I\ 28°6$$

$$\chi = 1 - A/A_{100}$$

where χ = degree of crystallinity, A = amorphous normalized diffraction, I 14°

TABLE II
Crystallization and Melting Temperatures from DSC Thermograms of POY Samples

Melting peak temp (°C)	Crystallization peak temp (°C)	Strain rate (min^{-1})	Straining temp (°C)
261	116	0.05	60
261	116	0.07	60
260	116	0.10	60
255–260	110	0.15	60
254–258	110	0.50	60
255–260	110	1.00	60
255–260	110	5.00	60
257–262	100	10.00	60
260	119	0.05	21
260	119	0.07	21
260	119	0.10	21
260	110	0.15	21
260	110	0.50	21
260	108	1.00	21
260	108	1.66	21
260	105	5.00	21
255–261	105	10.00	21
261	120	0.50	3
261	118	1.00	3
260	108	1.66	3
260	106	5.00	3
260–256	106	10.00	3
261	119	—	—

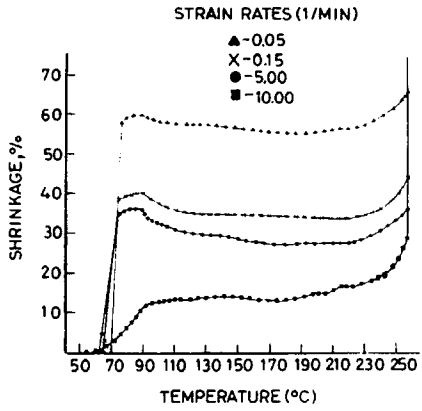

Fig. 6. Thermal retraction curves of POY samples strained at various strain rates at 21°C. Note: gradual changes from the typical amorphous into crystalline shape as the strain rate increases. Experimental error: $\Delta s = \pm 0.1\%$, $\Delta T = \pm 0.5°C$.

= amorphous diffraction intensity, I 28°6 = normalizing intensity, and A_{100} = normalized amorphous intensity of the reference sample which was an untreated POY.

Sonic Modulus

The Morgan dynamic modulus tester PPM5 was used to determine the T_g of the fibers by recording the changes in the degree of orientation with temperature. The yarns were stressed by weight to initial stresses of 0.1–0.01 g/denier. The tester with the yarn was placed into an oven with a controlled heating rate. The temperature was recorded by a thermocouple attached to the yarn. Changes in the degree of orientation were detected at the T_g by changes in the sound velocity following Moseley's theory of sound propagation in polymers.[33] Initial stress levels were chosen so as to enable the detection of the maximum shrinkage due to the disorientation at the T_g which expresses itself by a minimum in the sound velocity. Upon increasing the temperature, the stress due to the weight used increases the orientation and consequently the sound velocity.

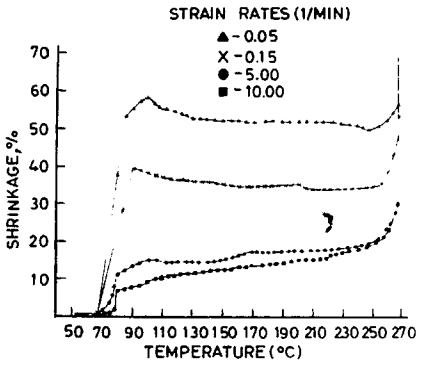

Fig. 7. Thermal retraction of POY samples strained at various strain rates at 60°C. Note: gradual changes from the typical amorphous into crystalline shape as the strain rate increases. Experimental error: $\Delta s = \pm 0.1\%$, $\Delta T = \pm 0.5°C$.

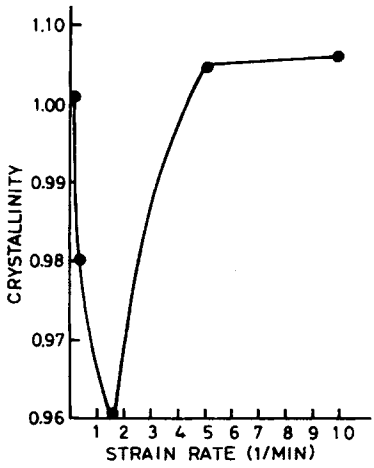

Fig. 8. DSC crystallinity vs. strain rate of POY samples strained at 80°C. Note: flow regime at strain rates <1.5 min^{-1}. Experimental error: $\Delta\chi = \pm 0.01$ cm^2/gm, Δ strain rate = ± 0.1 min^{-1}.

Stress–Relaxation

The technique used is based on a method given by Groenincky.[34] It measures the changes in relaxation modulus within 10 s at different temperatures. It has been shown[34] that T_i, the temperature of change in relaxation modulus, is related to T_g by ±3°C.

The yarns were wound in each case in 20 loops on the hooks mounted on the Instron. The hooks with the yarn were inserted into a silicone oil bath heated at a constant rate of 6°C/min. The temperature near the yarn and the shrinkage stresses were recorded and plotted as relaxation modulus vs. temperature.

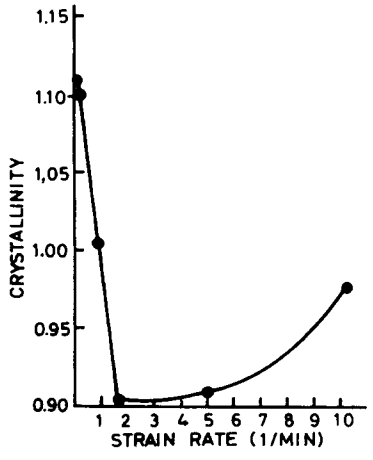

Fig. 9. DSC crystallinity vs. strain rate of POY samples strained at 92°C. Note: flow regime at strain rates 1.5 min^{-1}. Strain-induced crystallization regime at strain rates 1.5 min^{-1}. Experimental error: Δ strain rate = ± 0.1 min^{-1}.

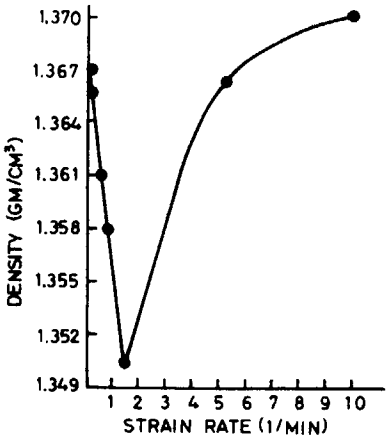

Fig. 10. Density vs. strain rates of POY samples strained at 80°C. Note: flow regime at strain rates <1.5 min^{-1}. Strain-induced crystallization regime at strain rates >1.5 min^{-1}. Experimental error: $\Delta\rho = \pm 0.0001$ gm/cm^3, Δ strain rate = ± 0.1 min^{-1}.

RESULTS AND DISCUSSION

Preliminary findings of strain-induced crystallization and T_g shift were obtained from thermal retraction and DSC experiments. The retraction thermograms are given in Figure 1. In fully oriented yarns (FOY) (C) there is a broad distribution of crystalline size and perfection which results in a continuous increase in the degree of shrinkage between the T_g and the melting point (T_m), which is characterized by excessive shrinkage due to the melting of relatively large and stable crystals. POY (A) is a highly oriented amorphous material; therefore all the orientation is released at the T_g. In cold-stretched POY (B) the amorphous phase loses its orientation at the T_g while the crystalline phase loses its orientation only at the T_m.

At the intermediate temperatures a substantial crystallization on uniaxially oriented nuclei is predominant up to 180°C and causes extension of the yarns.

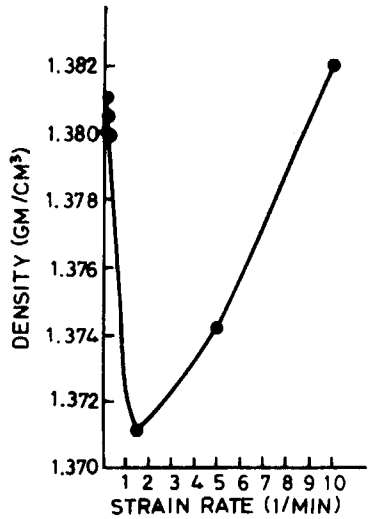

Fig. 11. Density vs. strain rate of POY samples strained at 92°C. Note: flow regime at strain rates 1.5 min^{-1}. Strain-induced crystallization regime at strain rates 1.5 min^{-1}. Experimental error: $\Delta = \pm 0.0001$ gm/cm^3. Δ strain rate = ± 0.1 min^{-1}.

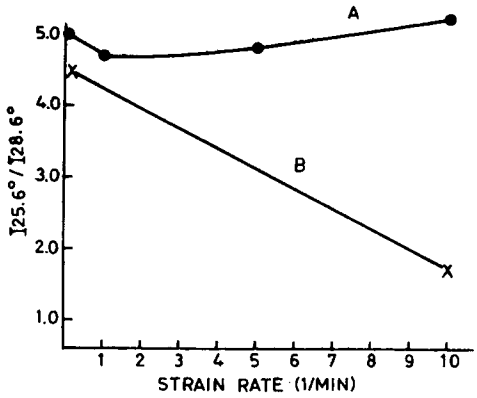

Fig. 12. Bosley's index of crystallinity vs. strain rates of POY samples: (A) strained at 80°C; (B) annealed at 80°C for time corresponding to the straining times in A. Experimental error: ΔI 25°6/I 28°6 = ±0.01, Δ strain rate = ±0.1 min^{-1}.

At temperatures above 180°C the excessive shrinkage offsets the crystallization effects and the yarn shrinks back to the level possessed at T_g and then to higher levels.

It was concluded from the retraction thermograms (Fig. 1) of the three samples that the cold-stretching process forms a distinct crystalline phase in the amorphous oriented fibers.

The DSC thermograms of the three samples (Fig. 2) show an exothermic peak around 90°C in the cold-strained POY. This is the temperature of the onset of elongation in the retraction thermograms. It appears therefore that the elongation is related to a crystallization process. The size of the exothermic peak of the cold-strained yarn, relative to POY shows that crystallization had taken

TABLE III

T_g Values by Sonic Modulus and Stress–Relaxation Techniques of POY Samples Strained below T_g

Sonic Modulus		Stress–Relaxation		Sample	
$T_g(l)$ (°C)	$T_g(u)$ (°C)	$T_g(l)$ (°C)	$T_g(u)$ (°C)	Strain rate (min^{-1})	Straining temp (°C)
52	72	52	73	0.50	3
49	76	48	74.5	1.00	3
44	78	43	78	1.66	3
41	78	42	78	5.00	3
37	78	40	78	10.00	3
39	69	37	70	12.00	21
—	69	—	65	—	—

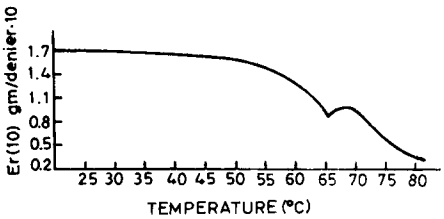

Fig. 13. Stress relaxation thermogram of untreated POY. Note: T_g = 65°C.

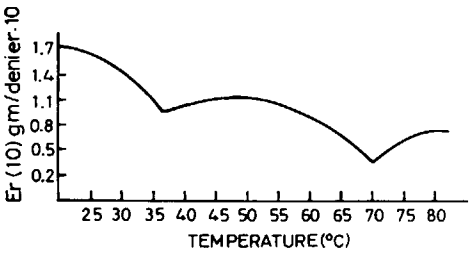

Fig. 14. Stress relaxation thermogram of POY that was strained at 21°C. Strain rate: 12.00 min^{-1}. Note: $T_g(l)$ = 37°C, $T_g(u)$ = 70°C.

place during the straining process. In FOY there is no further noticeable crystallization.

It is seen from the thermal retraction curves of the cold-strained POY that the shrinkage starts at a temperature lower by 40°C than in the case of the untreated POY or of the FOY. Identifying the temperature of the onset of shrinkage as the T_g[10,13] one may conclude that cold straining shifts T_g to lower temperatures.

Strain-Induced Crystallization

The yarn samples were strained at different rates in the range of 0.05–12.00 min^{-1}, and at different temperatures above and below the T_g. The straining below T_g took place at 3°C, 21°C, and 60°C.

The WAXD results are summarized in Table I and Figure 3. It is seen that the higher the strain rates, the larger the degree of crystallinity obtained and that the higher the temperature of straining, the more crystallinity is induced at the same strain rates.

Typical D.S.C. thermograms are shown in Figures 4, 5: Figure 4 shows thermograms of yarn strained at 60°C and strain rates of 0.05 min^{-1}. Note: No crystallization exotherm and a split of the melting endotherm. Figure 5 shows a thermogram of yarn strained at 3°C and strain rate of 10.00 min^{-1}. Note: Low crystallization exotherm and a wide melting endotherm. The DSC results are summarized in Table II and Figures 4 and 5. It is evident that the exothermic peak of the crystallization shifts from ca. 100°C to lower temperatures and has lower intensities as the strain rate or the temperature increase. Above a certain strain rate a split melting endotherm peak is observed. At higher temperatures the split of the melting endotherm peak starts at lower strain rates (see Table II).

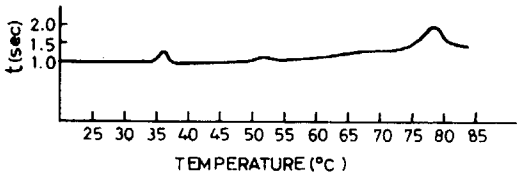

Fig. 15. Sound velocity thermogram of POY that was strained at 3°C. Strain rate: 10.00 min^{-1}. Note: $T_g(l)$ = 37°C, $T_g(u)$ = 78°C.

Thermal Retraction Studies

Figures 6 and 7 show gradual changes from the typical amorphous into crystalline shapes of thermograms as the strain rate of the samples increases. In the 21°C set, shown in Figure 6, the curves have more of the amorphous type character, i.e., a higher shrinkage at T_g. The yarns which were strained at higher rates at 60°C (Fig. 7) have more of the crystalline character than those that were strained at 21°C (Fig. 6).

It can be concluded that straining POY below T_g induces crystallization in the yarns. The closer the temperature to T_g and the higher the strain rates, the more the crystallization is induced.

Straining experiments above T_g are summarized in Figures 8 and 10 (80°C) and in Figures 9 and 11 (92°C). Two regimes can be observed at the two straining temperatures: In the slow strain rates regime (strain rate <1.5 min^{-1}) the degree of crystallinity is reduced as the strain rate increases. In the fast strain rate regime (strain rate >1.5 min^{-1}) the degree of crystallinity is increased as the strain rate increases.

The boundary between the regimes in both cases is the strain rate of 1.5 min^{-1}. At 92°C the degree of crystallinity is higher than those obtained at 80°C. Spruiell et al.[18] found, for amorphous PET strained at the same temperatures and strain rates, two regimes similarly separated by the same strain rate of 1.5 min^{-1}: they defined the slow strain rates as the flow regime and the high strain rates as the strain-induced crystallization regime.

Comparing Spruiell's results to ours reveals that in amorphous PET the degree of crystallinity increases slowly in the flow regime, and sharply in the strain induced crystallization regime. In POY, however, the degree of crystallinity is reduced in the flow regime and increases in the high strain rates regime. The difference shows the strong tendency of POY for thermal crystallization.

As the strain rate is increased, the time during which the yarn is subjected to the crystallization temperature (crystallization time) is reduced; therefore, the total degree of crystallinity becomes lower as the strain rate increases. In the strain-induced crystallization regime, the reduction of crystallization time is compensated by the process of strain induced crystallization and, therefore, the total degree of crystallinity increases as the strain rate increases. The point is further illustrated in Figure 12 in which Bosley's index of crystallinity of yarns strained at 80°C at different rates are given in curve A. These are compared (curve B) with indices obtained for yarns which were crystallized without straining at constant length for periods of time corresponding to the highest and lowest strain rates (25.0 and 0.2 min^{-1}). The difference between the two curves is due to strain-induced crystallization which occurs at the higher strain rates (strain-induced crystallization regime). Therefore, at low strain rates mainly thermal crystallization takes place. At high strain rates thermal and strain-induced crystallization occur simultaneously.

It is seen from Figures 9 and 11 that the density and the DSC crystallization changes similarly in the low strain range (flow regime). In the strain-induced crystallization regime, however, the DSC crystallinity at 92°C increases less and at a slower rate than the density crystallinity. This may be explained by assuming, following Bouriot et al.,[21] the formation of a mesomorphic phase with an intermediate degree of order, which causes a considerable increase in density with no accompanying increase in DSC crystallinity at the higher temperatures in the 80–100°C range.[35]

Glass Transitions of Strained POY

The T_g values of POY samples, strained to the natural draw ratio at different rates and at temperatures below T_g, are summarized in Table III and Figures 13, 14, and 15. It is seen that the untreated POY exhibits a single T_g value both by sonic modulus (69°C) and by stress–relaxation (65°C).

Upon cold straining at 21°C as well as at 3°C an increase in the T_g value from 65–69°C to 70–78°C was obtained. Furthermore, an additional glass transition in the lower temperature range of 37–52°C was observed.

Using the terminology of Boyer[23] the samples thus exhibit an upper $T_g(u)$ and a lower $T_g(l)$, and the higher the strain rate and the lower the straining temperature, the larger the difference between them.

We assume that the two glass transitions which differ by ca. 40°C, are probably due to formation of two distinct amorphous phases with different degrees of order, where the loose phase gives $T_g(l)$ while the compact phase is responsible for $T_g(u)$.[23]

The special conditions of cold straining at high speeds create the morphology of dense "mesomorphic" or "smectic" regions[21,22] alongside loose regions, which were presumably formed by the excess volume gained from the compact phase. When thermal energy is applied, the fiber tends to crystallize and to form stable structures which destroy the special metastable morphology required for the double T_g to appear. It appears therefore that in order to obtain the two glass transitions in POY, the straining should take place at temperatures much below the T_g of the untreated fiber.

References

1. Dror Selivansky and Menachem Lewin, The 45th Annual Meeting of the Israel Chemical Society, Abstracts AP-4, AP-5, June 19–20, 1978.
2. G. Lopatin, *J. Appl. Polym. Sci.*, **31**, 127–132 (1977).
3. I. Jacob and H. R. Schroder, *Chemifasern/Text ilindustrie* **38/82**, 228–232 (1980).
4. H. M. Heuvel and R. Huisman, *J. Appl. Polym. Sci.*, **22**, 2229–2243 (1978).
5. G. M. Venkatesh, A. H. Khan, P. J. Bose, and G. L. Madam, *J. Appl. Polym. Sci.*, **25**, 1601–1618 (1980).
6. J. O. Warwicker and B. Vevers, *J. Appl. Polym. Sci.*, **25**, 977–995 (1980).
7. L. Addyman and G. D. Ogilivie, *Br. Polym. J.*, **11**, 151–154 (1979).
8. R. M. Ikeda, *J. Polym. Sci., Polym. Lett.*, **18**, 325–331 (1980).
9. G. C. Adams, *Polym. Eng. Sci.*, **19**, 456–461 (1979).
10. D. E. Bosley, *J. Polym. Sci.*, **C20**, 77–107 (1967).
11. M. P. W. Wilson, *Polymer*, **15**, 277–282 (1974).
12. G. M. Bhatt and J. P. Bell, *J. Polym. Sci., Phys. Ed.* **14**, 575–590 (1976).
13. S. Lee and R. Simha, *Micromolecules*, **7**, 909–913 (1974).
14. A. B. Thompson, in *Fiber Structure*, J. W. Hearle and R. H. Peters, Ed., Butterworth, Washington, D.C., 1963, p. 105.
15. I. Marshall and A. B. Thompson, *Proc. R. Soc. London, A*, **221**, 545–562 (1954).
16. I. Marshall and A. B. Thompson, *J. Appl. Chem.*, **4**, 145–153 (1954).
17. A. B. Thompson, *J. Polym. Sci.*, **34**, 741–760 (1959).
18. J. E. Spruiell, D. E. McCord, and R. A. Beuerlein, *Trans. Soc. Rheol.*, **16**, 535–555 (1972).
19. R. P. Sheldon, *Polymer*, **4**, 213–219 (1963).
20. A. Misra, R. S. Stein, *J. Polym. Sci.*, **17**, 235–257 (1979).
21. P. Bouriot, B. Chabert, R. Hagege, G. Nemoz, and N. Valentin, *Bull. Sci. Inst. Text. France*, **9**, 37–51 (1980).
22. M. Sotton, A. M. Arniaud and C. Rabourdin, *J. Appl. Polym. Sci.*, **22**, 2585–2608 (1978).
23. R. F. Boyer, *J. Polym. Sci. Symp.*, **50**, 189–242 (1975).

24. N. P. C. Chao, J. A. Cucolo, A. R. Gallant, and T. W. George, *Appl. Polym. Symp.*, **27,** 193–204 (1975).
25. N. P. C. Chao, J. A. Cucolo, and T. W. George, *Appl. Polym. Symp.*, **27,** 175–192 (1975).
26. K. H. Illers and H. Bruer, *J. Colloid Sci.*, **18,** 1–31 (1963).
27. E. Ito and T. Hatakayama, *J. Polym. Sci., Phys. Ed.*, **12,** 1477–1483 (1974).
28. L. Nicolais and A. T. Dibenedetto, *J. Appl. Polym. Sci.*, **15,** 1585–1598 (1971).
29. C. C. Yau, Ph.D. thesis, North Carolina State University, Raleigh, 1972.
30. Tecam Density Gradient Column Model DC-1.
31. D. E. Bosley, *J. Appl. Polym. Sci.*, **8,** 1521–1529 (1964).
32. J. H. Dumbleton and B. B. Bowels, *J. Polym. Sci., A-2*, 951–958 (1966).
33. W. W. Mosley, *J. Appl. Polym. Sci.*, **3,** 266–276 (1960).
34. G. Groenincky, H. Reynaers, and H. Berghmans, *Polymer*, **15,** 61–62 (1974).
35. G. Hinrichen, H. G. Adam, H. Krebs, and H. Springer, *Coll. Polym. Sci.*, **258,** 232–240 (1980).

Received September 19, 1981
Accepted December 17, 1981